

# 基于人工神经网络的激光冲击复合强化 残余压应力预测与分布调控

周远航<sup>1,2</sup>, 冯爱新<sup>2\*</sup>, 韦朋余<sup>3</sup>, 张若楠<sup>3</sup>, 宋培龙<sup>3</sup>, 盛永琦<sup>2</sup>, 姚红兵<sup>1\*</sup>

(1.河海大学 力学与工程科学学院, 南京 210024; 2.温州大学瑞安研究生院,  
浙江 瑞安 325200; 3.中国船舶科学研究中心, 江苏 无锡 214000)

**摘要:** **目的** 通过结合人工神经网络和激光冲击有限元仿真,以减少激光冲击强化最佳参数设计的迭代次数,提高参数优化效率。**方法** 构建基于冲击波压力幅值的激光冲击强化 Abaqus 有限元模型。采用 Vdload 子程序与对应二次开发脚本形成光斑重叠区域残余应力的初始数据集。建立人工神经网络(ANN)算法模型,采用测试集对 ANN 模型进行测试,对超参数进行优化,对比分析不同机器学习算法的  $R^2$  得分、MAE 和 RMSE。设计并优化镍铝青铜模型表面的残余应力大小与分布,对比分析经机器学习预测后的模型表面残余应力分布情况。**结果** 经 ANN 预测整个面 LSCP 处理的模型表面形成了高达-413 MPa 的残余压应力,并且预测了均匀与非均匀的残余压应力分布;RMSE 均方根误差仅为 1.189 1,既显示出较好的预测精度,又避免了模型的过拟合,保证了一定的泛化能力,模型综合性能远优于其他经典的 ML 算法回归模型。所预测的残余压应力分布模型均达到了较深的影响层深,且在 1 Hz 的脉冲重复频率下,最大效率达到了 1.87 mm<sup>2</sup>/s。**结论** 激光冲击强化与机器学习的结合实现了易产生残余应力孔洞的镍铝青铜光斑重叠区域的最大残余压应力分布,且该方法优化出了整个表面的均匀与相对非均匀的残余压应力分布,为非均匀塑性应变引起镍铝青铜材料异质结构的形成开辟了新的设计途径。

**关键词:** 激光冲击复合强化; 人工神经网络; 复合强化; 残余应力

**中图分类号:** V261 **文献标志码:** A **文章编号:** 1001-3660(2024)13-0075-09

**DOI:** 10.16490/j.cnki.issn.1001-3660.2024.13.008

## Artificial Neural Network-based Prediction and Regulation of Residual Compressive Stress Distribution in Laser Shock Peening

ZHOU Yuanhang<sup>1,2</sup>, FENG Aixin<sup>2\*</sup>, WEI Pengyu<sup>3</sup>, ZHANG Ruonan<sup>3</sup>,  
SONG Peilong<sup>3</sup>, SHENG Yongqi<sup>2</sup>, YAO Hongbing<sup>1\*</sup>

(1. College of Mechanics and Engineering Science, Hohai University, Nanjing 210024, China; 2. Rui'an Graduate College, Wenzhou University, Zhejiang Rui'an 325200, China; 3. China Ship Scientific Research Center, Jiangsu Wuxi 214000, China)

**ABSTRACT:** Laser shock composite peening (LSCP) is one of the advanced methods for material surface enhancement, and it

收稿日期: 2024-05-04; 修订日期: 2024-07-06

**Received:** 2024-05-04; **Revised:** 2024-07-06

**基金项目:** 浙江省自然科学基金 (LY20E050027)

**Fund:** The Natural Science Foundation of Zhejiang Province (LY20E050027)

**引文格式:** 周远航, 冯爱新, 韦朋余, 等. 基于人工神经网络的激光冲击复合强化残余压应力预测与分布调控[J]. 表面技术, 2024, 53(13): 75-83.

ZHOU Yuanhang, FENG Aixin, WEI Pengyu, et al. Artificial Neural Network-based Prediction and Regulation of Residual Compressive Stress Distribution in Laser Shock Peening[J]. Surface Technology, 2024, 53(13): 75-83.

\*通信作者 (Corresponding author)

has gained significant attention recently due to its ability to induce beneficial residual stress fields. Traditional LSCP design methods involve selecting processing parameters through trial and error, which can be imprecise and time-consuming. These methods suffer from the complexities of internal stress wave transmission and non-uniform plastic strain under high strain rate loads. Machine learning (ML) algorithms offer a promising alternative by automating the design of critical LSCP parameters, thus reducing the iterative design process and associated costs. The work aims to leverage an Artificial Neural Network (ANN) algorithm to predict and regulate the residual compressive stress distribution on nickel-aluminum bronze surfaces, thus reducing the iterative design process and associated costs. An initial dataset of residual stresses in the spot overlap area was generated by an Abaqus finite element model with the Vdload subroutine and custom scripts. Before the regression analysis, the interquartile range (IQR) method was used to remove the top and bottom 10% of outliers, and the input data were standardized to eliminate the effect of data scale on the prediction results. The ANN model was trained and tested with the generated residual stress dataset, optimizing its hyperparameters for enhanced performance. Based on the process parameters in the training set, the residual stress values in areas prone to stress hole were predicted for 110 different process parameter sets. The results showed that almost all predictions were in close agreement with the actual values, confirming the strong prediction capability of the artificial neural network. The ANN accurately predicted residual compressive stress distributions, achieving an RMSE of 1.189 1, significantly outperforming other classical ML algorithms. The residual stress distributions were predicted and optimized, with the ANN model indicating compressive stress up to  $-413$  MPa across the treated surface. These predictions were validated by the test set, confirming the high prediction accuracy and robustness of the model against overfitting. Further analysis revealed that the predicted residual compressive stress distributions reached substantial effect depths, critical for material property enhancement. The LSCP process achieved a maximum efficiency of  $1.87\text{ mm}^2/\text{s}$  at a 1 Hz pulse repetition frequency. This method presents a novel approach to designing and regulating complex residual stress fields in LSCP, effectively addressing the challenge of residual stress hole in nickel-aluminum bronze. The integration of ML with LSCP not only optimizes the residual stress distributions, but also provides insights into the development of heterogeneous structures in the material due to non-uniform plastic strain. Future research will aim to incorporate more experimental data into the ML models to enhance their applicability to various types of metals and further refine the prediction accuracy of residual stress fields in complex material systems. This will involve collecting data from a broader range of experimental conditions and materials, thereby improving the robustness and versatility of the ML models. The goal is to create a comprehensive framework that can be applied to a wide array of materials and LSCP scenarios, ensuring that the benefits of this approach can be realized across different industries. This study contributes to the field of material surface enhancement by demonstrating the potential of combining advanced computational models with machine learning for more precise and efficient material treatment outcomes.

**KEY WORDS:** laser shock composite peening; artificial neural network; composite strengthening; residual stress

激光冲击复合强化应用于航空航天、海工核工等领域,进而引起了人们的广泛关注<sup>[1-5]</sup>。其具有高能、高压、超快等特征,是极端环境下的先进制造方法之一<sup>[6-8]</sup>。激光冲击复合强化利用高能激光辐照附着在材料表层的能量吸收层,在极短的时间内发生爆炸,爆炸产生的冲击波被约束层约束在一定的空间内,反作用于材料表面,材料表面因此产生极高应变率的塑性应变,从而达到表面残余应力调控的目的<sup>[9-10]</sup>。然而,激光冲击复合强化非均匀光斑引起的复杂应力场,尤其是在光斑搭接区域,极易产生应力孔洞区域,应力孔洞区域存在大量的拉应力<sup>[11-16]</sup>。材料表面的残余拉应力对材料来说是灾难性的,在极端载荷下往往是最初始被破坏的区域,特别是在材料表面承受交变载荷时,这种拉应力区域,往往是产生疲劳裂纹的扩展源,进而加速材料的疲劳失效,造成十分严重的安全事故<sup>[17-20]</sup>。

为了避免残余应力孔洞的产生,最大限度地减少材料表面因非均匀塑性应变产生的残余拉应力,研究人员在设计激光冲击复合强化试验时,通常会根据自己的经验调整各个参数,以获得最佳的残余应力场分布<sup>[21-25]</sup>。然而,激光冲击强化通常伴随着极其复杂的应力场变化过程,研究者很难基于这些应力场的变化来分析参数之间的内在联系,从而实现方向参数优化<sup>[26-28]</sup>。而如果充分考虑各个因素来设计激光冲击复合强化各个参数往往耗费大量的时间,并且很难确定参数是否已达最佳值。可见,探明激光冲击波加载下材料表面复杂的应力场变化过程,复合机器学习与激光冲击强化过程参数,快速实现方向参数的优化,是当前激光冲击复合强化领域亟待解决的关键问题之一。

幸运的是,机器学习的快速发展为解决这一挑战提供了可能性<sup>[29]</sup>。ML通过分原始数据集,识别出其中的有价值信息,并基于这些信息做出智能决策来完

成特定任务。近年来一系列结合了 ML 的创新模型已经在激光增材制造<sup>[30]</sup>、声子超材料<sup>[31]</sup>与激光冲击强化<sup>[32-33]</sup>等领域展现了其独特的能力,有效地减少设计与模拟时间成本<sup>[34-38]</sup>。然而,对于激光冲击强化过程中复杂的残余应力场的预测与调控,特别是残余应力孔洞区域的预测,仍然十分具有挑战性。

针对上述问题,本研究提出了一种通过复合深度学习(DL)算法与激光冲击强化有限元分析方法进行应力场调控的激光冲击复合强化(LSCP)新方法。采用人工神经网络(ANN)算法学习并且预测易发生应力孔洞区域的残余应力,以及相应的最优工艺参数,从而实现应力场的调控,明显避免了应力孔洞的产生且在易发生应力孔洞的区域形成了残余压应力分布。探究了 5 种最大残余压应力模型下激光冲击参数与应力应变的影响规律,以阐明激光冲击波加载下残余应力孔洞的调控机制。

## 1 模型与理论

### 1.1 LSCP 有限元模型构建

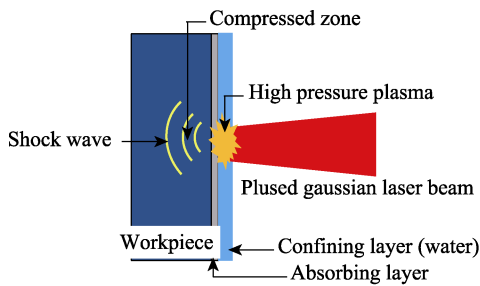
#### 1.1.1 激光冲击波加载模型构建

激光冲击波加载过程为复杂的物理过程,本文采用 R-Fabro<sup>[39]</sup>膨胀模型对其进行描述,将激光冲击波压强加载过程描述为:

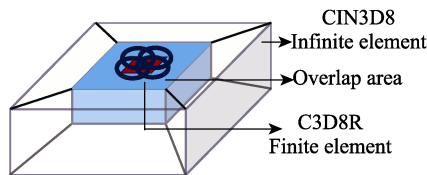
$$P = 0.01 \sqrt{\frac{2\alpha}{3(2\alpha+3)}} \times \sqrt{Z} \times \sqrt{I_0} \quad (1)$$

在空间上,以高斯光束加载形式加载。选择坐标原点为激光光斑的中心,冲击波压力的非均匀空间分布描述为:

$$P(x, y, z) = P(t) \exp\left(-\frac{x^2 + y^2}{2R^2}\right) \quad (2)$$



a LSCP原理图



b LSCP有限元模型示意图

在时间上,一个激光加载周期内冲击波压力分布描述为:

$$P(t) = \begin{cases} P_{\max} \cdot -0.01(t-20)t, & 0 \text{ ns} < t < 10 \text{ ns} \\ P_{\max} \cdot \exp[-0.3(t-10)], & 10 \text{ ns} \leq t \leq 20 \text{ ns} \end{cases} \quad (3)$$

此外,为了消除相邻脉冲加载下应力波的叠加影响且考虑到减少计算时间,相邻脉冲加载间隔设置为 1 μs。为了消除首脉冲不稳定性的影响,采用首脉冲抑制的方法,首脉冲 Load 0 被抑制,从 Load 1 开始加载第 1 个光斑。

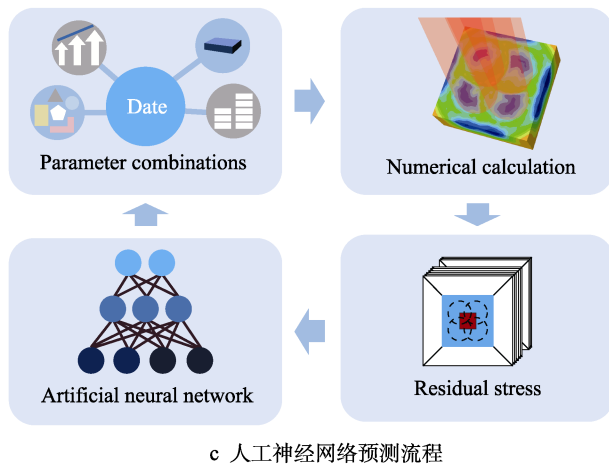
#### 1.1.2 有限元分析模型构建

在上述高斯光束加载时空分布模型构建的基础上,采用 ABAQUS 有限元分析软件配合二次开发子程序 Vdload 以及对应 Python 脚本实现模拟过程,总体有限元模型尺寸为 15 mm×15 mm×5 mm,将有限元模型分为 2 个部分,内部设置尺寸为 8 mm×8 mm×3 mm 的冲击区域,网格单元设置为 C3D8R 有限单元,网格单元尺寸设置为 0.16 mm;其余区域设置为 CIN3D8 无限单元,以阻止应力波在材料内部的反射与干涉(图 1b)。

激光冲击波加载过程中,其原理是利用几十纳秒短脉冲、高峰值功率密度(约 10<sup>9</sup> W/cm<sup>2</sup>)激光束辐照金属材料表面,产生极高的压强(可达 GPa),材料表面发生极高应变率塑性应变(10<sup>6</sup> s<sup>-1</sup>)<sup>[40]</sup>。同时金属表面的吸收层具有隔热作用,材料的塑性应变可以看作是冷变形,材料表面只受到冲击波压力作用。采用 J-C 本构方程<sup>[41]</sup>来对弹塑性力学行为进行描述,见式(4)。

$$\sigma = (A + B\varepsilon^n) \left[ 1 + C \ln \left( \frac{\dot{\varepsilon}}{\dot{\varepsilon}_0} \right) \right] \left[ 1 - \left( \frac{T - T_0}{T_m - T_0} \right)^m \right] \quad (4)$$

式中:  $\varepsilon$  表示塑性应变;  $\dot{\varepsilon}/\dot{\varepsilon}_0$  是无量纲塑性应变



c 神经网络预测流程

图 1 神经网络预测残余应力流程

Fig.1 Artificial neural network prediction process for residual stress: a) schematic diagram of LSCP principle; b) schematic diagram of LSCP finite element model; c) artificial neural network prediction process

率;  $A$ 、 $B$  为常数, 反映了材料的应变硬化特征;  $C$  为反应应变率对材料性能的影响。仿真所采取的镍铝青铜物理力学性能参数<sup>[42]</sup>见表 1。

表 1 所采用的镍铝青铜 J-C 本构物理力学性能参数  
Tab.1 Physico-mechanical properties of the  
nickel-aluminum bronze J-C constitutive model used

$\rho/$ ( $\text{g}\cdot\text{cm}^{-3}$ )	Young's modulus/ MPa	$A/$ MPa	$B/$ MPa	Poisson's ratio	$C$	$n$	$m$
7.64	121 000	295	759.5	0.34	0.002 1	0.405	1.09

## 1.2 人工神经网络算法与激光冲击参数的链接

建立 LSCP 工艺参数与残余应力场分布之间的定量关系是利用 ANN 预测 LSCP 工艺参数的先决条件。在确定激光加载的时空分布模型与有限元网格模型后, 通过试错程序确定 LSCP 峰值压强、重叠率、光斑直径、冲击次数 4 个变量参数的允许范围 (表 2)。根据不同的 LSCP 工艺参数, 生成了 1 008 个 LSCP 工艺参数与光斑重叠区域残余应力的数据集作为原始的数据集。选择 LSCP 4 个参数作为人工神经网络的输入参数, 将易发生残余应力孔洞区域 (图 1b 红色区域) 的残余应力平均值指定为输出参数。测试集的划分比例为 0.05, 使用训练集训练人工神经网络模型, 随后在训练后使用独立的测试集进行测试。利用人工神经网络模型预测工艺参数进行有限元仿真计算 (图 1c), 附带 10% 的误差允许范围, 若超过误差允许阈值, 则新生成的数据引入初始数据集, 随后重新开始神经网络训练, 通过多次迭代, 提高神经网络系统的预测精度。

表 2 预测残余应力特征变量与最小精度  
Tab.2 Predicted residual stress feature variables and  
minimum accuracy

LSCP parameter	Parameter range	Minimum accuracy
$P_{\max}/\text{MPa}$	2 000-8 000	1 750
Overlap/%	20-80	10
$R/\text{mm}$	0.5-2	0.5
Times	1-7	1

## 2 ML 模型构建与分析

### 2.1 ANN 预测模型结构设计

本研究利用全连接人工神经网络来预测易发生参与应力孔洞区域的残余应力。人工神经网络的配置由输入层、标准化层、隐藏层与输出层组成。在回归分析前, 采用四分位距法移除前后 10% 的异常值, 对输入数据进行标准化转换, 以消除数据尺度对预测结

果的影响<sup>[43]</sup>。神经网络的隐藏层包括 20、200、200、10 个神经元, 学习率设置为 0.001。为了提升模型的泛化能力, 减少模型对单个数据点的依赖, 促使神经网络学习更加健壮的特征, 避免过拟合, 每层神经元之间采用 Dropout 函数临时丢弃随机的神经元, 丢弃比率设置为 0.3。此外, 为了保持一定的网络梯度流, 维持神经网络中更多神经元的活跃性, 每层神经元之间采用 LeakyReLU 函数<sup>[44]</sup>作为激活函数, 正斜率设置为 0.01。图 2b~c 显示了不同迭代次数下, 训练集与测试集的损失函数与  $R^2$ , 表明模型展现出出色的拟合能力和最小的泛化误差。

在人工神经网络模型经过训练后, 采用测试集对其进行验证。依据训练集中的工艺参数, 预测了 110 组不同工艺参数下易发生应力孔洞区域的残余应力值。预测值和真实值之间的比较分析如图 2d 所示, 从图中数据对比可以发现, 几乎所有的测试值都与真实值接近一致, 证实了人工神经网络强大的预测能力。在此之后利用梯度特征归因法<sup>[46]</sup> (Gradient Feature Attribution) 计算在当前模型预测值和实际值之间的损失函数, 以评估各个工艺参数对光斑重叠区域残余应力的影响权重。结果表明, 所选取的特征自变量均展现出一定的贡献度, 表明自变量选取合理。另外, LSCP 冲击次数与峰值压强对光斑重叠区域的残余应力影响更大。

### 2.2 与其他 ML 方法比较

为了评估 ANN 回归模型在残余应力预测中的性能, 线性回归模型 (Linear Regression, LR)、支持向量机模型 (Support Vector Machine, SVM)、K 近邻模型 (K-Nearest Neighbors, KNN)、轻量级梯度提升机模型 (Light Gradient Boosting Machine, Light GBM) 与随机森林 (Random Forest) 被用作进行比较, 这些算法已广泛应用于结构设计、参数优化、数据处理等领域。在测试过程中, 测试集的尺度仍选择 0.05, 并通过网格搜索获得每种算法的最优超参数, 以确保每个回归模型都是最优的。表 3 显示了不同算法模式下残余应力的预测结果。结果表明, ANN 算法有着较低的 MAE 和 RMSE, 同时具备着较高的  $R^2$ , 与其他的经典算法模型相比, 在残余应力的预测中表现出更好的稳定性和更高的精准度。

## 3 结果与讨论

采用 ANN 预测的 5 种光斑重叠区域最大残余应力值所对应的工艺参数, 开展了表面更大区域的激光强化仿真研究。图 3 显示了 ANN 回归模型得到的不同工艺参数下材料整个表面的残余应力与应变的分布情况, 模型表面均显示出了较大的残余压应力, LSCP 所表现出的表面残余压应力分别达到了



-369、-370、-413、-240、-144 MPa, 接下来将从各个方面评估高应变率所产生的残余压应力, 包括表面残余应力分布情况、激光冲击的效率、深度方向应力分布情况的比较。

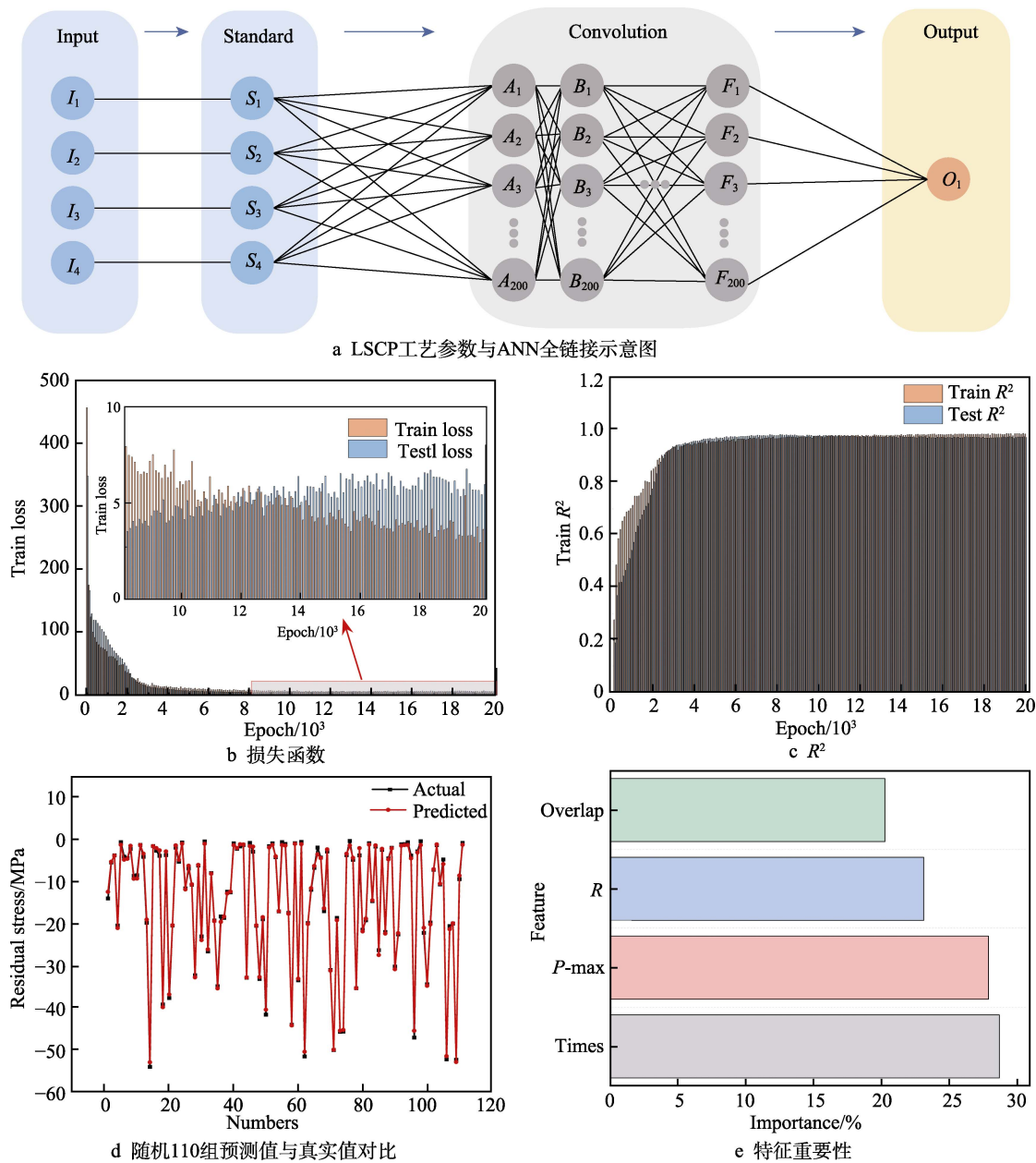


图 2 基于人工神经网络设计误差分析及预测结果  
Fig.2 Artificial neural network-based design error analysis and prediction results: a) schematic diagram of LSCP process parameters and full connection in ANN; b) loss function; c)  $R^2$ ; d) comparison of predicted and actual values for a random set of 110; e) feature importance

表 3 几种经典算法模式下残余应力的预测结果  
Tab.3 Comparison of predicted residual stress results by various classic algorithmic approaches

Types of algorithms	$R^2$ score	MAE	RMSE	Predicted value	Actual value	APE
LR	0.292	10.014	12.035	-35.764	-18.811	441.1
SVM	0.551	7.397	9.592	-31.773	-47.407	267.1
KNN	0.535	5.889	9.778	-41.898	-1.093	210.3
Light GBM	0.941	2.304	3.478	-45.537	-44.789	81.9
RF	0.921	2.476	4.027	-43.674	-47.407	84.98
ANN	0.982	1.182 4	1.189 7	-46.54	-47.407	32.6

### 3.1 表面残余应力分布情况分析

图 3a~e 显示了 LSCP 后模型表面应力分布情况, 材料表面均呈现出较大的残余压应力, 部分模型在非常小的区域仅存在着几十兆帕的残余拉应力, 从图中还发现部分模型表面呈现较均匀的残余应力分布, 而另外部分模型表面呈现出非常明显的非均匀性。图 3f~i 为 LSCP 后模型表面的应变情况, 与光斑加载和应力分布呈现一致的规律。结合激光冲击的工艺参数可以得出, 光斑重叠率为 60% 时 (图 3a、f), 表面呈现出了较为均匀的残余压应力分布; 而当光斑重叠率低至 40% 时 (图 3b、g), 过低的重叠率导致了模型

中心光斑重叠区域光斑数量较少, 表面应力分布趋于紊乱, 且存在着 60 MPa 左右的残余拉应力, 这对材料的强化是不利的。值得注意的是, 当光斑搭接率为 50%、激光加载峰值压强为 7 250 MPa、冲击次数为 5 时, 模型表面生成了较大的残余压应力, 且表面光斑作用区域无拉应力产生。

选取相对均匀与相对非均匀压应力分布 2 种模型, 对表面 5 条路径上的表面应力进行了统计分析。图 4 为所选取的 5 条路径以及路径上模型表面的残余应力分布状况, 相对于图 4b, 图 4a 显示出相对均匀的残余压应力分布且路径上存在着少量的残余拉应力, 实现了相对均匀的残余应力分布的调控。图 4b

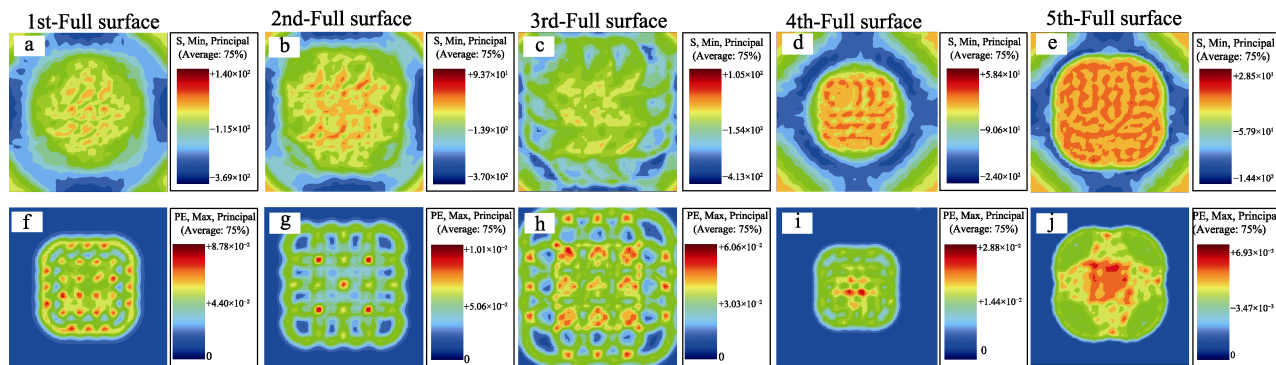


图 3 ANN 回归模型预测整个表面的残余应力与应变的分布情况

Fig.3 Distribution of residual stress and strain across the entire surface predicted by the ANN regression model

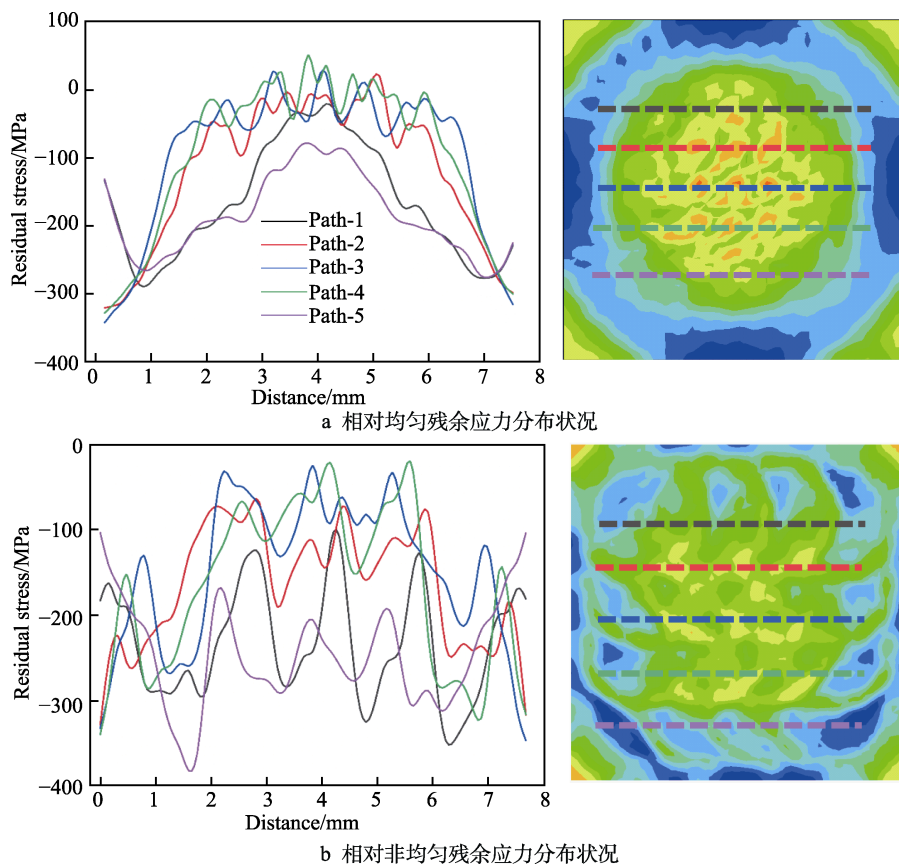


图 4 5 条路径上模型表面的残余应力均匀分布状况

Fig.4 Uniform distribution of residual stress on the model surface along five paths: a) relatively uniform residual stress distribution; b) relatively non-uniform residual stress distribution

显示出相对较大的非均匀性,同时也形成了大范围的残余压应力,在多晶材料的冲击强化中,这种非均匀塑性应变对于材料的应力调控是有利的。

### 3.2 几种参数下激光冲击强化效率对比情况分析

激光冲击复合强化时,决定激光冲击复合强化效率的分别取决于光斑重叠率、光斑直径、重复频率与冲击次数。其内在关系可总结为:

$$\eta = \frac{2r + 2r(1-o)}{f \cdot n} \quad (5)$$

式中:  $\eta$  为激光冲击复合强化效率;  $r$  为光斑半径;  $o$  为光斑重叠率;  $f$  为重复频率, 设置为 1 Hz;  $n$  为光斑的个数。所采用的面积为与 4 个光斑相切的正方形面积 (图 5a 中橘色区域)。图 5b 显示了 ANN 模型预测的各工艺参数的 LSCP 加工效率, 在 1 Hz 的频率下, 最大效率达到了 1.87 mm<sup>2</sup>/s, 此时光斑作用

区域的残余应力分布 (图 3e、j) 为压应力分布。

### 3.3 深度方向残余应力分析

图 6 为相对均匀表面应力分布和非均匀表面应力分布 2 种情况下深度方向的残余应力分布情况, 在模型的表层为急性变形区域, 呈现出显著的残余压应力分布; 次表层为轻微变形区域, 呈现出明显的拉应力状态。图 6b 中显示出与光斑加载方式有关的规律性, 而图 6a 中与光斑加载方式的关联性不显著, 这是由于在高重叠率情况下, 光斑与光斑的多次叠加造成一个光斑与另一个光斑之间相互影响的规律性逐渐消失。图 6c 和图 6d 为 2 种工艺参数下模型深度方向的应变情况, 均匀表面应力分布情况下 (图 6c) 的影响层深度小于非均匀表面应力分布的影响层深度 (图 6d), 这是由于更高能量与更多次数的激光脉冲加载, 传入至模型的总能量足够大, 使得影响层深度更深。

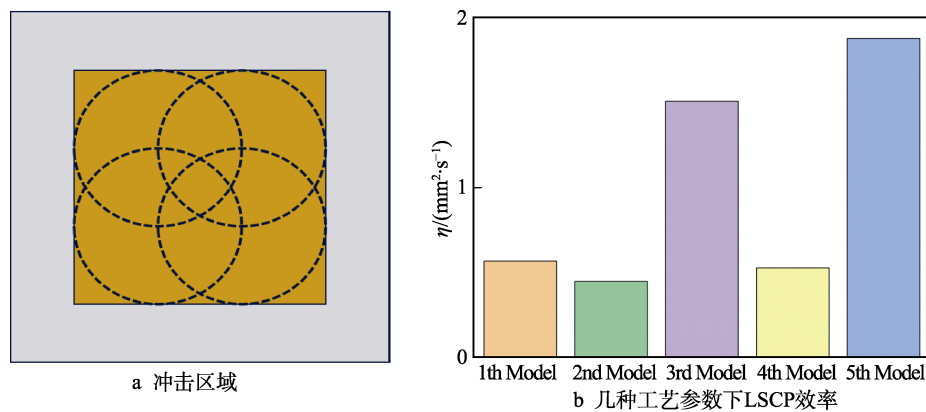


图 5 ANN 回归模型预测的 LSCP 参数效率对比情况  
Fig.5 Comparison of LSCP parameter efficiency predicted by the ANN regression model: a) impact area; b) LSCP efficiency under various process parameters

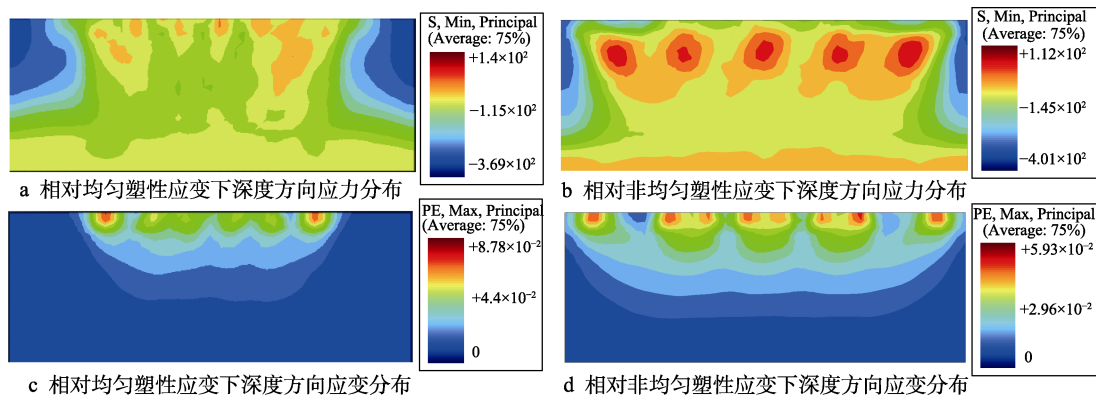


图 6 LSCP 模型深度方向应力应变云图

Fig.6 Stress and strain contour maps in the depth direction of the LSCP model: a) relatively stress distribution under uniform plastic strain; b) relatively stress distribution under non-uniform plastic strain; c) relatively strain distribution under uniform plastic strain; d) relatively strain distribution under non-uniform plastic strain

## 4 结论

综上所述,激光冲击强化与机器学习的复合实现

了易产生残余应力孔洞的镍铝青铜光斑重叠区域的最大残余压应力分布。针对不同的可调参数构建了 ANN 回归预测模型,以找到最佳的激光冲击复合强

化模型参数。通过 ANN 回归模型预测最大的残余压应力,消除了传统手动设计过程中复杂且耗时的调整过程。ANN 回归模型的预测均方根误差在合理范围内为 1.189 7,既显示出较好的预测精度,又避免了模型的过拟合,保证了一定的泛化能力,模型综合性能远优于其他经典的 ML 算法回归模型。此外,预测的光斑重叠区域最大残余压应力可以优化出整个表面的均匀与相对非均匀的残余压应力分布,为材料表面的残余应力场调控提供了新的技术手段。当然,本研究存在一定的局限性,受制于有限元算法理论的局限性,本研究仅考虑了弹塑性力学模型,未将晶粒细化、位错以及晶界的滑移考虑在其中。未来研究可以在基于人工神经网络的激光冲击复合强化的基础上,不断加入仿真与实验的数据,从而获得更为精确的人工神经网络激光冲击预测模型。与传统表面应力调控手段相比,本文提出的 ML 的设计方法大大简化了设计过程,且模型表面呈现出优异的残余压应力值。该方法为激光冲击复合强化工艺参数的高精度设计开辟了一条新的途径。

## 参考文献:

- [1] 姚喆赫,潘成颢,迟一鸣,等. 超声复合激光制造技术研究进展(特邀)[J]. 中国激光, 2024, 51(4): 49-67.  
YAO Z H, PAN C H, CHI Y M, et al. Research Progress of Ultrasonic Assisted Laser Manufacturing Technology (Invited)[J]. Chinese Journal of Lasers, 2024, 51(4): 49-67.
- [2] WAN Z D, DAI W, GUO W S, et al. Improved Corrosion Resistance of Ni-Base Alloy 600 Welded Joint by Laser Shock Peening[J]. Journal of Manufacturing Processes, 2022, 80: 718-728.
- [3] 聂祥樊,李阳,王亚洲,等. 飞机结构激光冲击强化研究进展与展望[J]. 航空学报, 2023, 44(24): 35-56.  
NIE X F, LI Y, WANG Y Z, et al. Research Progress and Prospect of Laser Shock Peening Technology in Aircraft Structure[J]. Acta Aeronautica et Astronautica Sinica, 2023, 44(24): 35-56.
- [4] PAVAN M, FURFARI D, AHMAD B, et al. Fatigue Crack Growth in a Laser Shock Peened Residual Stress Field[J]. International Journal of Fatigue, 2019, 123: 157-167.
- [5] ZHANG H P, CAI Z Y, CHI J X, et al. Fatigue Crack Growth in Residual Stress Fields of Laser Shock Peened Ti6Al4V Titanium Alloy[J]. Journal of Alloys and Compounds, 2021, 887: 161427.
- [6] HE Z R, SHEN Y Z, TAO J, et al. Laser Shock Peening Regulating Aluminum Alloy Surface Residual Stresses for Enhancing the Mechanical Properties: Roles of Shock Number and Energy[J]. Surface and Coatings Technology, 2021, 421: 127481.
- [7] 杨青天,张永康,池元清,等. 激光冲击对海洋工程用 E690 钢微观组织及性能的影响[J]. 表面技术, 2023, 52(11): 439-447.  
YANG Q T, ZHANG Y K, CHI Y Q, et al. Effect of Laser Peening on the Microstructure and Properties of E690 Offshore Steel[J]. Surface Technology, 2023, 52(11): 439-447.
- [8] BAI Y J, LYU G, WANG Y J, et al. Laser Shock Peening Strengthens Additively Manufactured High-Entropy Alloy through Novel Surface Grain Rotation[J]. Materials Science and Engineering: A, 2023, 871: 144886.
- [9] DENG W W, WANG C J, LU H F, et al. Progressive Developments, Challenges and Future Trends in Laser Shock Peening of Metallic Materials and Alloys: A Comprehensive Review[J]. International Journal of Machine Tools and Manufacture, 2023: 104061.
- [10] AYEB M, FRIJA M, FATHALLAH R. Prediction of Residual Stress Profile and Optimization of Surface Conditions Induced by Laser Shock Peening Process Using Artificial Neural Networks[J]. The International Journal of Advanced Manufacturing Technology, 2019, 100(9): 2455-2471.
- [11] LU G X, WANG L, LI H, et al. Methods for the Suppression of "Residual Stress Holes" in Laser Shock Treatment[J]. Materials Today Communications, 2021, 28: 102486.
- [12] LI K M, CAI Y, YU Z, et al. Formation Mechanism of Residual Stress Hole under Different Pulse Durations and Shock Pressure Distributions in Ti6Al4V Alloy during Laser Peen Texturing[J]. Optics & Laser Technology, 2020, 130: 106361.
- [13] WANG C, LI K F, HU X Y, et al. Numerical Study on Laser Shock Peening of TC4 Titanium Alloy Based on the Plate and Blade Model[J]. Optics Laser Technology, 2021, 142: 107163.
- [14] CAO Y P, WANG Z M, SHI W D, et al. Formation Mechanism and Weights Analysis of Residual Stress Holes in E690 High-Strength Steel by Laser Shock Peening[J]. Coatings, 2022, 12(2): 285.
- [15] 盛湘飞,谭慧勇,袁文志,等. 激光冲击诱导应力波对残余应力孔洞形成的影响[J/OL]. 表面技术, 2024: 1-15. (2024-04-16). <https://kns.cnki.net/kcms/detail/50.1083.TG.20240412.1619.014.html>.  
SHENG X F, TAN H Y, YUAN W Z, et al. Effect of Laser Shock Induced Stress Waves on the Formation of Residual Stress Holes[J/OL]. Surface Technology, 2024: 1-15. (2024-04-16). <https://kns.cnki.net/kcms/detail/50.1083.TG.20240412.1619.014.html>.
- [16] LU G X, WANG D G, GAO S, et al. Will the Laser Shock-Induced Residual Stress Hole Inevitably Occur?[J]. Journal of Materials Research and Technology, 2022, 18: 3626-3630.
- [17] WANG C Y, LUO K Y, BU X Y, et al. Laser Shock Peening-Induced Surface Gradient Stress Distribution and Extension Mechanism in Corrosion Fatigue Life of AISI 420 Stainless Steel[J]. Corrosion Science, 2020, 177: 109027.
- [18] BIKDELOO R, FARRAHI G H, MEHMANPARAST A, et al. Multiple Laser Shock Peening Effects on Residual Stress Distribution and Fatigue Crack Growth Behaviour

- of 316L Stainless Steel[J]. Theoretical and Applied Fracture Mechanics, 2020, 105: 102429.
- [19] TONG Z P, LIU H L, JIAO J F, et al. Improving the Strength and Ductility of Laser Directed Energy Deposited CrMnFeCoNi High-Entropy Alloy by Laser Shock Peening[J]. Additive Manufacturing, 2020, 35: 101417.
- [20] KALENTICS N, DE SEIJAS M O V, GRIFFITHS S, et al. 3D Laser Shock Peening - A New Method for Improving Fatigue Properties of Selective Laser Melted Parts[J]. Additive Manufacturing, 2020, 33: 101112.
- [21] KULIIEV R, KELLER S, KASHAEV N. Identification of Johnson-Cook Material Model Parameters for Laser Shock Peening Process Simulation for AA2024, Ti-6Al-4V and Inconel 718[J]. Journal of Materials Research and Technology, 2024, 28: 1975-1989.
- [22] LIU H L, YANG H J, TONG Z P, et al. Forming Quality and Residual Stress Analysis of Al2024-T351 Perforated Sheets with Laser Annulus and Strip Peening[J]. Optics Laser Technology, 2024, 171: 110333.
- [23] SHEN X J, SHUKLA P, SUBRAMANIYAN A K, et al. Residual Stresses Induced by Laser Shock Peening in Orthopaedic Ti-6Al-7Nb Alloy[J]. Optics & Laser Technology, 2020, 131: 106446.
- [24] GU C, SU M H, TIAN Z H, et al. Multi-Scale Simulation Study on the Evolution of Stress Waves and Dislocations in Ti Alloy during Laser Shock Peening Processing[J]. Optics & Laser Technology, 2023, 165: 109629.
- [25] QI S P, SHEN Y X. Numerical Investigation on Spall Fracture in Metallic Materials Due to Laser Shock Peening via Phase Field Approach to Fracture[J]. Engineering Fracture Mechanics, 2023, 292: 109598.
- [26] CAI S P, ZHANG Y K. An Iterative Approach Combined with Multi-Dimensional Fitting of Limited Measured Stress Points to Reconstruct Residual Stress Field Generated by Laser Shock Peening[J]. Surface and Coatings Technology, 2022, 436: 128237.
- [27] ZHOU W F, YANG Y, WU Y S, et al. Improving Fatigue Initiation Life of Open-Hole Fibre Metal Laminates by Laser Shock Peening[J]. Journal of Materials Research and Technology, 2024, 28: 2206-2218.
- [28] PARK E K, LEE H J, KIM J H, et al. Approximate Residual Stress and Plastic Strain Profiles for Laser-Peened Alloy 600 Surfaces[J]. Nuclear Engineering and Technology, 2023, 55(4): 1250-1264.
- [29] NI C C, LI S. Machine Learning Enabled Industrial IoT Security: Challenges, Trends and Solutions[J]. Journal of Industrial Information Integration, 2024, 38: 100549.
- [30] REN K, CHEW Y, ZHANG Y F, et al. Thermal Field Prediction for Laser Scanning Paths in Laser Aided Additive Manufacturing by Physics-Based Machine Learning[J]. Computer Methods in Applied Mechanics and Engineering, 2020, 362: 112734.
- [31] JI W, CHANG J, XU H X, et al. Recent Advances in Metasurface Design and Quantum Optics Applications with Machine Learning, Physics-Informed Neural Networks, and Topology Optimization Methods[J]. Light: Science & Applications, (n.d.). <https://www.nature.com/articles/s41377-023-01218-y> (accessed March 1, 2024).
- [32] WU J J, HUANG Z, QIAO H C, et al. Prediction about Residual Stress and Microhardness of Material Subjected to Multiple Overlap Laser Shock Processing Using Artificial Neural Network[J]. Journal of Central South University, 2022, 29(10): 3346-3360.
- [33] NIE X F, HE W F, CAO Z Y, et al. Experimental Study and Fatigue Life Prediction on High Cycle Fatigue Performance of Laser-Peened TC4 Titanium Alloy[J]. Materials Science and Engineering: A, 2021, 822: 141658.
- [34] PERAL-GARCÍA D, CRUZ-BENITO J, GARCÍA-PENALVO F J. Systematic Literature Review: Quantum Machine Learning and Its Applications[J]. Computer Science Review, 2024, 51: 100619.
- [35] LIU C X, YU G L, LIU Z L. Machine Learning Models in Phononic Metamaterials[J]. Current Opinion in Solid State and Materials Science, 2024, 28: 101133.
- [36] KARNIADAKIS G E, KEVREKIDIS I G, LU L, et al. Physics-Informed Machine Learning[J]. Nature Reviews Physics, 2021, 3: 422-440.
- [37] LIU K L, SHANG Y L, OUYANG Q, et al. A Data-Driven Approach with Uncertainty Quantification for Predicting Future Capacities and Remaining Useful Life of Lithium-Ion Battery[J]. IEEE Transactions on Industrial Electronics, 2021, 68(4): 3170-3180.
- [38] ESTERHUIZEN J A, GOLDSMITH B R, LINIC S. Interpretable Machine Learning for Knowledge Generation in Heterogeneous Catalysis[J]. Nature Catalysis, 2022, 5: 175-184.
- [39] PEYRE P, FABBRO R, MERRIEN P, et al. Laser Shock Processing of Aluminium Alloys. Application to High Cycle Fatigue Behaviour[J]. Materials Science and Engineering: A, 1996, 210(1/2): 102-113.
- [40] LU H, REN Y P, CHEN Y, et al. Wear Resistance of 20Cr2Ni4A Alloy Steel Treated by Laser Shock Peening and Implantation of Diamond Nanoparticles[J]. Surface and Coatings Technology, 2021, 412: 127070.
- [41] BRAISTED W. Finite Element Simulation of Laser Shock Peening[J]. International Journal of Fatigue, 1999, 21(7): 719-724.
- [42] FU Z T, YANG W Y, ZENG S Q, et al. Identification of Constitutive Model Parameters for Nickel Aluminum Bronze in Machining[J]. Transactions of Nonferrous Metals Society of China, 2016, 26(4): 1105-1111.
- [43] WERNER DE VARGAS V, SCHNEIDER ARANDA J A, DOS SANTOS COSTA R, et al. Imbalanced Data Preprocessing Techniques for Machine Learning: A Systematic Mapping Study[J]. Knowledge and Information Systems, 2023, 65(1): 31-57.
- [44] MANIATOPOULOS A, MITIANOUDIS N. Learnable Leaky ReLU (LeLeLU): An Alternative Accuracy-Optimized Activation Function[J]. Information, 2021, 12(12): 513.
- [45] ZHAO W M, ALWIDIAN S, MAHMOUD Q H. Adversarial Training Methods for Deep Learning: A Systematic Review[J]. Algorithms, 2022, 15(8): 283.